

Quantum Phase Transitions in the Bosonic Single-Impurity Anderson Model

Hyun-Jung Lee¹ and Ralf Bulla¹

¹*Theoretische Physik III, Elektronische Korrelationen und Magnetismus, Universität Augsburg, 86135 Augsburg, Germany*

(Dated: July 21, 2021)

We consider a quantum impurity model in which a bosonic impurity level is coupled to a non-interacting bosonic bath, with the bosons at the impurity site subject to a local Coulomb repulsion U . Numerical renormalization group calculations for this bosonic single-impurity Anderson model reveal a zero-temperature phase diagram where Mott phases with reduced charge fluctuations are separated from a Bose-Einstein condensed phase by lines of quantum critical points. We discuss possible realizations of this model, such as atomic quantum dots in optical lattices. Furthermore, the bosonic single-impurity Anderson model appears as an effective impurity model in a dynamical mean-field theory of the Bose-Hubbard model.

PACS numbers: 05.10.Cc (Renormalization Group methods), 05.30.Jp (Boson systems), 03.75.Nt (Other Bose-Einstein condensation phenomena), 03.75.Hh (Static properties of condensates).

The focus of this work is the physics of a bosonic impurity state coupled to a non-interacting bosonic environment modeled by the Hamiltonian

$$H = \varepsilon_0 b^\dagger b + \frac{1}{2} U b^\dagger b (b^\dagger b - 1) + \sum_k \varepsilon_k b_k^\dagger b_k + \sum_k V_k (b_k^\dagger b + b^\dagger b_k) . \quad (1)$$

The energy of the impurity level (with operators $b^{(\dagger)}$) is given by ε_0 ; the parameter U is the local Coulomb repulsion acting on the bosons at the impurity site. The impurity couples to a bosonic bath via the hybridization V_k , with the bath degrees of freedom given by the operators $b_k^{(\dagger)}$ with energy ε_k .

We term the system defined by eq. (1) the ‘bosonic single-impurity Anderson model’ (bosonic siAm), in analogy to the standard (fermionic) siAm [1] which has a very similar structure except that all fermionic operators are replaced by bosonic ones. Furthermore, we do not consider internal degrees of freedom of the bosons, such as the spin (an essential ingredient in the fermionic siAm).

There are various ways to motivate the study of the model eq. (1). From a purely theoretical point of view it is interesting to compare the physics of the fermionic and bosonic versions of the siAm. Of course, there are striking differences between these two models: there is no direct bosonic analog of local moment formation and screening of these local moments at low temperatures, characteristics of the fermionic Kondo effect [2]. On the other hand, the bosonic model allows for a Bose-Einstein condensation (BEC), at least in a certain parameter space (see Fig. 1 below), a phenomenon which is clearly absent in the fermionic model.

There are certain similarities between the fermionic and the bosonic model concerning the role of the local Coulomb repulsion U : increasing the value of U can induce a quantum phase transition from a phase with screened spin to a local moment phase in the fermionic case [3], while it can induce a quantum phase transition

from a BEC phase to a ‘Mott phase’ in the bosonic case, as shown below.

Another motivation for studying the bosonic siAm comes from a treatment of the Bose-Hubbard model within dynamical mean-field theory (DMFT) [4]. Although such an investigation has not been pursued so far, it is clear that the effective impurity model onto which the Bose-Hubbard model is mapped will have a similar form as eq. (1) (see also Ref. 5). An obvious application of such a DMFT treatment would then address the Mott transition in the Bose-Hubbard model [6] which must have its counterpart on the level of the effective impurity model – and the ‘Mott transition’ on the impurity level is precisely what we are looking at here.

Finally, a physical system described by the bosonic siAm could be directly realized in optical lattices, where the laser fields are tuned in such a way that a single ‘impurity’ site is formed within an approximately unperturbed lattice system (‘atomic quantum dots’, see Refs. 7, 8). Provided the Coulomb repulsion at all sites except the impurity can be neglected, the corresponding model can be directly mapped onto the model eq. (1). Present theoretical studies of atomic quantum dots focus, however, on a coupling between impurity and excitations of the superfluid environment [7], for which a description in terms of the spin-boson model is more appropriate.

For the calculations presented in this paper we use the numerical renormalization group (NRG) originally developed by Wilson for the Kondo problem [9]. This method has been shown to give very accurate results for a broad range of impurity models, including the fermionic siAm [1, 10] but also quantum impurities with coupling to a bosonic bath [11, 12]. Here we employ the bosonic extension of the NRG (bosonic NRG) to study the model eq. (1). We shall present ground state phase diagrams of the bosonic siAm, identify fixed points and discuss quantum phase transitions between the fixed points. Although far from comprehensive, our results indicate that the bosonic siAm shows a variety of interesting proper-

ties which deserve to be studied in greater detail in the future.

Before we come to the results from the bosonic NRG, let us discuss some general properties and trivial limits of the model eq. (1).

Similar to other quantum impurity models, the influence of the bath on the impurity is completely specified by the bath spectral function

$$\Delta(\omega) = \pi \sum_k V_k^2 \delta(\omega - \varepsilon_k) . \quad (2)$$

Here we assume that $\Delta(\omega)$ can be parametrized by a powerlaw for frequencies up to a cutoff ω_c (we set $\omega_c = 1$ in the calculations)

$$\Delta(\omega) = 2\pi \alpha \omega_c^{1-s} \omega^s, \quad 0 < \omega < \omega_c . \quad (3)$$

The parameter α is the dimensionless coupling constant for the impurity-bath interaction. This form of $\Delta(\omega)$ is certainly not the most general one and specific applications (within a bosonic DMFT or for an impurity level in an optical lattice) will lead to additional structures in $\Delta(\omega)$.

The NRG calculations can be both performed for a canonical and a grandcanonical ensemble. Here we present only results for a grandcanonical ensemble for which we set the chemical potential of the bath to $\mu = 0$. This means that a Bose-Einstein condensation of the whole system (impurity plus bath) can only be induced by the coupling to the impurity. This can already be understood from the non-interacting case, $U = 0$: here a direct diagonalization of the bosonic siAm shows that with increasing α , a localized state with *negative* energy separates out of the continuum at a critical value $\alpha = \alpha_c$. The BEC then occurs via populating this localized state, a feature which can also be observed in the numerical calculations.

The other trivial limit of the bosonic siAm is the decoupled impurity, $\alpha = 0$. The succession of quantum phase transitions as shown in Fig. 1 for $\alpha = 0$ can be easily understood from the dependence of the many-particle levels on the parameters ε_0 and U . The transition occurs for $\varepsilon_0/U = -n_{\text{imp}}$ when the energies of the states with n_{imp} and $n_{\text{imp}} + 1$ electrons are degenerate.

The full phase diagram Fig. 1 is calculated with the bosonic NRG [12]. In this approach, the frequency range of the bath spectral function $[0, \omega_c]$ is divided into intervals $[\omega_c \Lambda^{-(n+1)}, \omega_c \Lambda^{-n}]$, $n = 0, 1, 2, \dots$, with Λ the NRG discretization parameter (we use $\Lambda = 2.0$ for all the results shown in this paper). The continuous spectral function within these intervals is approximated by a single bosonic state and the resulting discretized model is then mapped onto a semi-infinite chain with the Hamiltonian

$$H = \varepsilon_0 b^\dagger b + \frac{1}{2} U b^\dagger b (b^\dagger b - 1) + V (b^\dagger \bar{b}_0 + \bar{b}_0^\dagger b)$$

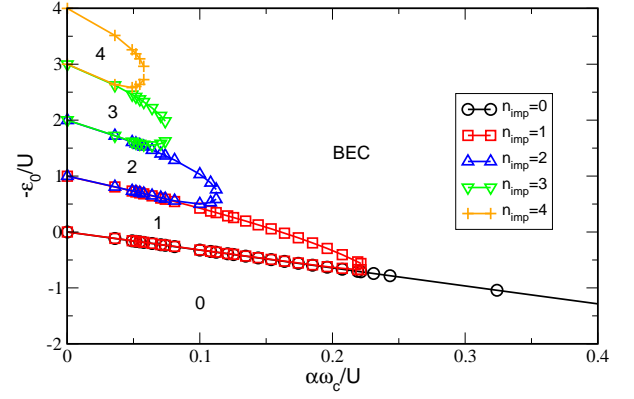


FIG. 1: Zero-temperature phase diagram of the bosonic siAm for bath exponent $s = 0.6$ and fixed impurity Coulomb interaction $U = 0.5$. The different symbols denote the phase boundaries between the Mott phases and the BEC phase. The Mott phases are labeled by their occupation n_{imp} for $\alpha = 0$. Only the Mott phases with $n_{\text{imp}} \leq 4$ are shown. The NRG parameters are $\Lambda = 2.0$, $N_b = 10$, and $N_s = 100$.

$$+ \sum_{n=0}^{\infty} \varepsilon_n \bar{b}_n^\dagger \bar{b}_n + \sum_{n=0}^{\infty} t_n \left(\bar{b}_n^\dagger \bar{b}_{n+1} + \bar{b}_{n+1}^\dagger \bar{b}_n \right) . \quad (4)$$

Here the impurity couples to the first site of the chain via the hybridization $V = \sqrt{2\alpha/(1+s)}$. The bath degrees of freedom are in the form of a tight-binding chain with operators $\bar{b}_n^{(\dagger)}$, on-site energies ε_n , and hopping matrix elements t_n which both fall off exponentially: $t_n, \varepsilon_n \propto \Lambda^{-n}$.

The chain model eq. (4) is diagonalized iteratively starting with the impurity site and adding one site of the chain in each iteration. As for the application to the spin-boson model, only a finite number N_b of basis states for the added site can be taken into account, and, after diagonalizing the enlarged cluster, only the lowest-lying N_s many-particle states are kept for the subsequent iterations (here we use $N_b = 10 - 20$ and $N_s = 100 - 200$). The main technical difference to the spin-boson model is that we can use the total particle-number as a conserved quantity in the Hamiltonian eq. (1). Furthermore, the renormalization group flow turns out to be considerably more stable as in the calculations for the spin-boson model so that we can easily perform up to $N = 100$ iterations (a detailed account of the technical details will appear elsewhere).

Let us now discuss the $T = 0$ phase diagram of the bosonic siAm, Fig. 1, calculated for fixed $U = 0.5$ with the parameter space spanned by the dimensionless coupling constant α and the impurity energy ε_0 . We choose $s = 0.6$ as the exponent of the powerlaw in $\Delta(\omega)$ (the s -dependence of the phase diagram is discussed in Fig. 4 below). The phase diagram is characterized by a sequence of lobes which we label by the impurity occupation n_{imp} at $\alpha = 0$ where it takes integer values. We use the terminology ‘Mott phases’ for these lobes, due to the appar-

ent similarity to the phase diagram of the Bose-Hubbard model. The Mott phases are separated from the BEC phase by lines of quantum critical points which terminate (for $s = 0.6$) at a finite value of α , except for the $n_{\text{imp}} = 0$ phase where the boundary extends up to infinite α . These transition can be viewed as the impurity analogue of the Mott transition in the lattice model, since it is the local Coulomb repulsion which prevents the formation of the BEC state.

The phase diagram Fig. 1 is deduced from the flow of the lowest-lying many-particle levels which allows quite generally to identify fixed points and transitions between these fixed points [10]. Figure 2 shows the flow for $s = 0.4$, fixed $\alpha = 0.007$ and $U = 0.5$, and two values of ε_0 very close to the quantum phase transition. The solid lines belong to the Mott phase with $n_{\text{imp}} = 2$ and display a crossover between two fixed points: from an unstable quantum critical point for iteration numbers $N \sim 20 - 40$ to a stable fixed point for $N > 70$. Analysis of the stable fixed point shows that it can be described by a decoupled impurity with occupation $n_{\text{imp}} = 2$ and a free bosonic bath given by the decoupled chain. (The actual impurity occupation, however, differs from the integer values, as discussed below.) The structure of the quantum critical point, on the other hand, is presently not clear but might be accessible to perturbative methods as discussed in [13].

The dashed lines belong to the BEC phase where, apparently, something dramatic is happening at $N \approx 55$. The divergence of the energies for all excited states seen in this plot is due to the formation of a localized state, split off from the continuum by an energy gap Δ_g , very similar to the behavior for $U = 0$. This energy gap takes a finite value which is not renormalized to zero as Λ^{-N} as the levels of the other fixed points, therefore the divergence of $\Delta_g \cdot \Lambda^N$. In the inset of Fig. 2 we plot E_N (instead of $E_N \Lambda^N$) so that the development of the gap $\Delta_g \approx 4 \times 10^{-18}$ appears as a plateau of the first excited state. The extremely small value of the gap is due to the tuning of the parameters very close to the transition (Δ_g vanishes at the transition).

Further analysis of the data shows that the ground state in the BEC phase has an occupation number given by the maximum boson number used in the iterative diagonalization.

The fact that the unstable fixed point separating the Mott phase from the BEC phase is indeed a quantum critical point can be deduced from its non-trivial level structure, as mentioned above, and the behavior of the crossover scale T^* . Numerically we find that upon variation of ε_0 close to its critical value $\varepsilon_{0,c}$, the crossover scale vanishes with a powerlaw at the transition, $T^* \propto |\varepsilon_0 - \varepsilon_{0,c}|^\nu$ on both sides of the transition, with a non-trivial exponent $\nu \approx 2.50 \pm 0.06$. This exponent is observed for all lines of quantum critical points for fixed $s = 0.4$ and preliminary results show that $\nu = 1/s$ for $0 < s < 1$.

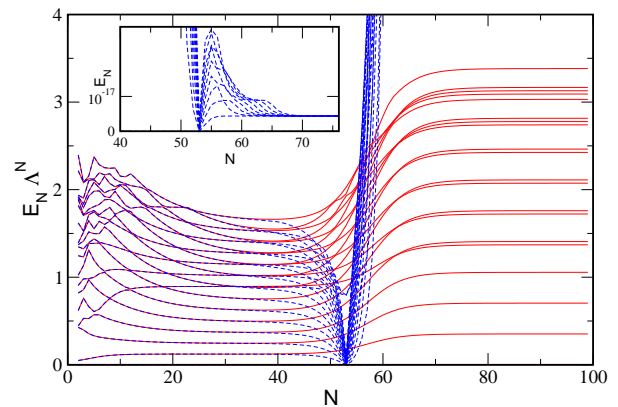


FIG. 2: Flow diagram of the lowest lying many-particle levels E_N versus iteration number N for parameters $s = 0.4$, $\alpha = 0.007$, $U = 0.5$, and two values of ε_0 very close to the quantum phase transition between the Mott phase with $n_{\text{imp}} = 2$ and the BEC phase. Both the quantum critical point and the Mott phase appear as fixed points in this scheme whereas in the BEC phase, a gap Δ_g opens between the ground state and the first excited state, see the inset where E_N (instead of $E_N \Lambda^N$) is plotted versus N .

Let us now focus on the impurity occupation n_{imp} for temperature $T = 0$. Figure 3 shows the dependence of n_{imp} on ε_0 for $s = 0.4$, $U = 0.5$, and various values of α . The symbols indicate that the parameters lie within the Mott phase whereas the crosses are for the BEC phase. Both sets of lines form a continuous curve but it is unclear at the moment whether the data in the BEC phases are reliable (due to the special features in the flow diagram discussed above).

The terminology we use here suggests an integer occupation throughout the Mott phase, as for the Bose-Hubbard model, but for the bosonic siAm n_{imp} deviates from the integer values as soon as the coupling to the bath is finite, see Fig. 3. This is to be expected since for a gapless bath spectral function $\Delta(\omega)$, the charge fluctuations on the impurity site cannot be completely suppressed. Indeed we observe that for increasing the value of the bath exponent s , the $n_{\text{imp}}(\varepsilon_0)$ -curve gets closer to the step function. At this point one can speculate about the possible development of $\Delta(\omega)$ in a DMFT treatment of the Mott phase. The self-consistency might generate a bath spectral function with a gap and the impurity occupation might then turn into the step function expected for the lattice model.

The precise shape of the boundaries in the phase diagram Fig. 1 depends on the form of $\Delta(\omega)$ for *all* frequencies. Here we stick to the powerlaw form eq. (3) and present the dependence of the phase diagram on the bath exponent s in Fig. 4. We observe that upon increasing the value of s , the areas occupied by the Mott phases extend to larger values of α and significantly change their shape. A qualitative change is observed when the exponent approaches $s = 1$. First of all, the Mott phases appear

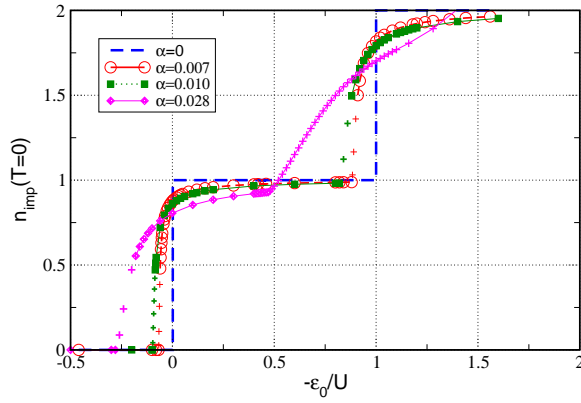


FIG. 3: Impurity occupation n_{imp} as a function of ε_0 for temperature $T = 0$, $s = 0.4$, $U = 0.5$, and various values of α . The sharp steps for the decoupled impurity $\alpha = 0$ are rounded for any finite α . Symbols (crosses) correspond to data points within the Mott (BEC) phases.

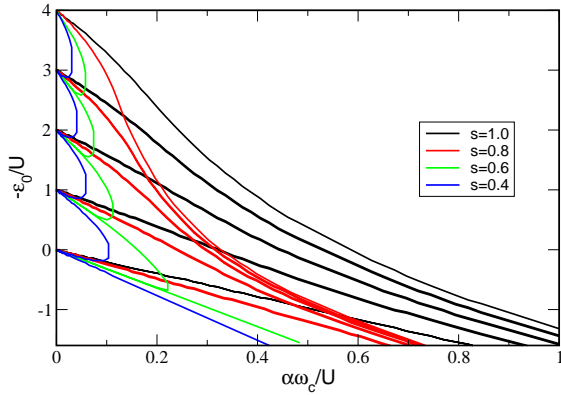


FIG. 4: Zero-temperature phase diagram of the bosonic siAm as in Fig. 1, but now for different values of the bath exponent s . For increasing value of s , the areas occupied by the Mott phases significantly change their shape and for $s = 1$ it appears that each Mott phase extends up to arbitrarily large values of α .

to extend up to arbitrarily large values of α . Furthermore, the BEC phase which separates the Mott phases for $s < 1$ and $\alpha > 1$ is completely absent for $s = 1$! We do not yet have an explanation for this observation and it would be interesting to find out whether the absence of the BEC phase is due to the special form of $\Delta(\omega)$, eq. (3), or whether it is a generic feature even when $\Delta(\omega) \propto \omega$ is only valid for $\omega \rightarrow 0$.

The case $s = 0$ (constant bath density of states) turns out to be difficult to access numerically. An extrapolation of the phase boundaries for values of s in the range $0.1 \dots 0.4$ to $s = 0$ is inconclusive, but the Mott phase is at least significantly suppressed in this limit.

To summarize, we have presented NRG calculations for the phase diagram and the impurity occupation of a bosonic version of the single-impurity Anderson model. The phase diagram contains Mott phases, in which the local Coulomb repulsion prevents Bose-Einstein conden-

sation, separated by the BEC phase by lines of quantum critical points. The studies presented here are only the starting point for a comprehensive investigation of the bosonic siAm and we are planning to calculate, for example, physical properties at finite temperatures and dynamic quantities (impurity spectral function and self-energy). The latter will be of importance for a possible DMFT for the Bose-Hubbard model, an approach which has not yet been fully developed due to various conceptual problems. One issue is the proper scaling of the Hamiltonian parameters in the limit of infinite spatial dimensions [14]. For example, the model on a hypercubic lattice as studied in Ref. 15 requires a scaling of the hopping matrix elements as $1/d$ which leads to a static mean-field theory. In addition, the bosonic DMFT in the superfluid phase of the Bose-Hubbard model might generate a more complex impurity model, the bosonic siAm introduced here would then be applicable only within the Mott phases of the lattice model.

Finally, it would be interesting to identify situations for atomic quantum dots in optical lattices which can be described by the bosonic single-impurity Anderson model.

We would like to thank Krzysztof Byczuk, Jim Freericks, Matthias Vojta, and Dieter Vollhardt for helpful discussions. This research was supported by the DFG through SFB 484.

-
- [1] A. C. Hewson, *The Kondo Problem to Heavy Fermions* (Cambridge Univ. Press, Cambridge 1993).
 - [2] A bosonic analogue of the Kondo effect can be observed in the models proposed in S. Florens, L. Fritz, and M. Vojta, Phys. Rev. Lett. **96**, 036601 (2006); these models are not directly related to the bosonic siAm studied here.
 - [3] Such a quantum phase transition is seen, for example, in the soft-gap Anderson and Kondo models, see M. Vojta, Phil. Mag. **86**, 1807 (2006), and references therein.
 - [4] For the DMFT for fermionic models, see W. Metzner and D. Vollhardt, Phys. Rev. Lett. **62**, 324 (1989); A. Georges, G. Kotliar, W. Krauth, and M. J. Rozenberg, Rev. Mod. Phys. **68**, 13 (1996).
 - [5] R. Bulla, Phil. Mag. **86**, 1877 (2006).
 - [6] M. P. A. Fisher, P. B. Weichman, G. Grinstein, and D. S. Fisher, Phys. Rev. B **40**, 546 (1989).
 - [7] A. Recati, P. O. Fedichev, W. Zwerger, J. von Delft, and P. Zoller, Phys. Rev. Lett. **94**, 040404 (2005).
 - [8] D. Jaksch and P. Zoller, Ann. of Phys. **315**, 52 (2005).
 - [9] K. G. Wilson, Rev. Mod. Phys. **47**, 773 (1975).
 - [10] H. R. Krishna-murthy, J. W. Wilkins, and K. G. Wilson, Phys. Rev. B **21**, 1003 (1980); *ibid.* **21**, 1044 (1980).
 - [11] R. Bulla, N.-H. Tong, and M. Vojta, Phys. Rev. Lett. **91**, 170601 (2003).
 - [12] R. Bulla, H.-J. Lee, N.-H. Tong, and M. Vojta, Phys. Rev. B **71**, 045122 (2005).
 - [13] H.-J. Lee, R. Bulla, and M. Vojta, J. Phys.: Condens. Matter **17**, 6935 (2005).
 - [14] D. Vollhardt, private communication.
 - [15] J. K. Freericks and H. Monien, Phys. Rev. B **53**, 2691 (1996).